ACADEMIC PRESS

Available online at www.sciencedirect.com

SCIENCE DIRECT®

Journal of Sound and Vibration 262 (2003) 677–705

JOURNAL OF SOUND AND VIBRATION

www.elsevier.com/locate/jsvi

Application of a generalized residual model to frequency domain modal parameter estimation

William A. Fladung, Allyn W. Phillips*, Randall J. Allemang

Structural Dynamics Research Laboratory (SDRL), University of Cincinnati, P.O. Box 210072, Cincinnati, OH 45221-0072, USA

Received 28 January 2002; accepted 10 January 2003

Abstract

Residuals have long been used in frequency domain parameter estimation methods to model the influence of out-of-band modes but, typically, as a fixed set of no more than two or three terms. Recently, a systematic approach to the use of residual polynomials has led to the development of a generalized residual model. The use of a generalized residual model with rational fraction polynomial frequency domain parameter estimation methods allows the contribution of out-of-band modes to be included without increasing the model order and creating additional computational poles. Of particular interest is the use of the generalized residual for single-degree-of-freedom (s.d.o.f.) techniques, which generally do not consider the residual effects and suffer accordingly. With the use of generalized residuals, it becomes possible to properly account for nearby modes and also extract accurate residues with an s.d.o.f. algorithm. The development of the generalized residual polynomial model is outlined and a new s.d.o.f. frequency domain algorithm with generalized residuals is developed.

1. Introduction

The frequency response of a system is the superposition of an infinite number of individual modes that have contribution at all frequency. Residuals are simplified expressions included in the frequency response model to account for the influence of modes outside the frequency range of interest. Residuals have been included in all types of frequency domain algorithms for estimating poles and residues, but primarily as a byproduct or afterthought. However, residuals are an integral part of the rational fraction polynomial parameter estimation model. This paper proposes

*Corresponding author. Tel.: +1-513-556-2720; fax: +1-513-556-3390.
E-mail address: allyn.phillips@uc.edu (A.W. Phillips).

0022-460X/03/$ - see front matter
doi:10.1016/S0022-460X(03)00117-2

that the numerator polynomial, which describes the residues and residuals, and the denominator polynomial, which describes the poles, are equally important in the parameter estimation process.

2. Background

Modal parameter estimation is as "a special case of system identification where the a priori model of the system is known to be in the form of modal parameters [1]". The multiple-input/multiple-output (MIMO) frequency response function (FRF) model can be formulated as the partial fraction, or modal model

$$[H(\omega)] = \sum_{r=1}^{\bar{N}} \left(\frac{[A_r]}{\mathrm{j}\omega - \lambda_r} + \frac{[A_r^*]}{\mathrm{j}\omega - \lambda_r^*} \right), \tag{1}$$

which is non-linear in the unknown parameters, the poles (λ_r) and the residues (A_r). The problem can also be approached in two linear stages as the rational fraction polynomial model

$$[H(\omega)] = \frac{\sum_{k=0}^{\bar{m}-2} (\mathrm{j}\omega)^k [\beta_k]}{\sum_{k=0}^{\bar{m}} (\mathrm{j}\omega)^k [\alpha_k]}, \quad \text{where } \bar{m} \geqslant 2 \tag{2}$$

from which the poles are computed as the eigenvalues of the companion matrix formed with the $[\alpha_k]$ coefficient matrices. Once the poles are known, the solution for the residues in Eq. (2) is linear.

Modal parameter estimation involves separating the single-degree-of-freedom contributions to the multiple-degree-of-freedom (m.d.o.f.) frequency response function measurements using numerical techniques [1]. The summation of s.d.o.f. modes to form an m.d.o.f. FRF, which is stated mathematically in Eqs. (1) and (2) and is depicted graphically in Fig. 1, where the dotted lines are the s.d.o.f. modes and the solid line is the m.d.o.f. summation.

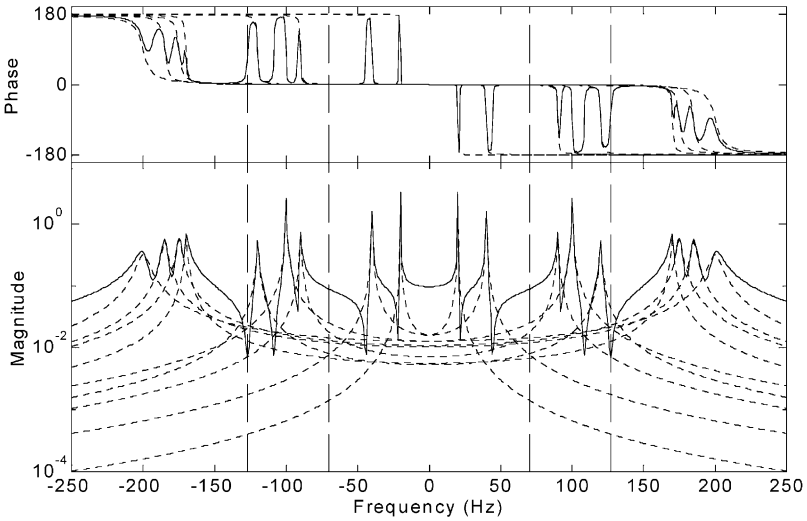

Fig. 1. Superposition of s.d.o.f. modes to form an m.d.o.f. FRF.

In both forms of the MIMO FRF model in Eqs. (1) and (2) above, it is implicit that all modes are included, but in reality, the FRFs are measured in some frequency range. In addition, the data are often processed in limited frequency bands of interest. The vertical, dashed lines in Fig. 1 depict the positive- and negative-frequency ranges of interest.

The FRF models can be written in three frequency bands, with modes in the frequency range of interest and upper and lower out-of-band modes, in partial fraction form as

$$[H(\omega)] = \underbrace{\sum_r \frac{[A_r]}{\mathrm{j}\omega - \lambda_r}}_{\text{lower out-of-band modes}} + \underbrace{\sum_r \frac{[A_r]}{\mathrm{j}\omega - \lambda_r}}_{\text{in-band modes}} + \underbrace{\sum_r \frac{[A_r]}{\mathrm{j}\omega - \lambda_r}}_{\text{upper out-of-band modes}} \tag{3}$$

or in rational fraction form as

$$[H(\omega)] = \underbrace{\frac{\sum_k (\mathrm{j}\omega)^k [\beta_k]}{\sum_k (\mathrm{j}\omega)^k [\alpha_k]}}_{\text{lower out-of-band modes}} + \underbrace{\frac{\sum_k (\mathrm{j}\omega)^k [\beta_k]}{\sum_k (\mathrm{j}\omega)^k [\alpha_k]}}_{\text{in-band modes}} + \underbrace{\frac{\sum_k (\mathrm{j}\omega)^k [\beta_k]}{\sum_k (\mathrm{j}\omega)^k [\alpha_k]}}_{\text{upper out-of-band modes}} . \tag{4}$$

With regard to the positive- and negative-frequency bands, the terms of upper and lower out-of-band modes should be considered in the absolute-value sense, while the in-band modes also include the contributions of their conjugates. The lower and upper out-of-band modes are considered as residuals with respect to the frequency range of interest and are included in the models as simplified expressions:

$$[H(\omega)] = [R_l(\omega)] + \sum_{r=1}^{N} \left(\frac{[A_r]}{\mathrm{j}\omega - \lambda_r} + \frac{[A_r^*]}{\mathrm{j}\omega - \lambda_r^*} \right) + [R_u(\omega)] \tag{5}$$

and

$$[H(\omega)] = [R_l(\omega)] + \frac{\sum_{k=0}^{m-2} (\mathrm{j}\omega)^k [\beta_k]}{\sum_{k=0}^{m} (\mathrm{j}\omega)^k [\alpha_k]} + [R_u(\omega)], \tag{6}$$

where $[R_l(\omega)]$ is the lower residual function and $[R_u(\omega)]$ is the upper residual function. Note that the N in Eq. (5), the number of modes in the frequency range of interest, is different from the $\bar{N}$ in Eq. (1), the total number of system modes, and that the m in Eq. (6) is different from the $\bar{m}$ in Eq. (2).

As indicated in Eqs. (3)–(6), residuals are terms included in the frequency response model to account for the contributions of modes that are above and below the frequency range of interest. Residuals are typically classified as lower residuals, which represent the contribution of the modes below the frequency range of interest, and as upper residuals, which represent the contribution of the modes above the frequency range of interest. The most commonly used expression for the lower residual is an inverse function of frequency squared and for the upper residual is a constant. Residuals have been included in algorithms that estimate poles, such as those developed in Refs. [2–26] and in algorithms that estimate residues or mode shapes, such as those in Refs. [12,14–16,19,23,27–30]. In addition, the residuals themselves have been estimated for use in system modelling application, such as in Refs. [31–37], or for Hilbert transform procedures, as in Ref. [38]. Some of the earliest developments of residuals in the modal area were by Klosterman [39] in

1971, followed by Van Loon [40] in 1974. Since then the development of most frequency domain parameter estimation algorithms have included some consideration of residuals.

The use of residuals is generally restricted to frequency domain models because the effects of out-of-band modes are not readily described in the time domain. In the frequency domain, the contribution of the modes below, above and within the frequency range of interest can be naturally separated and simplified expressions for the residuals formulated. But in the time domain, both the modes of interest and the residual modes have response at all time points. That is, the response of in-band and out-of-band modes cannot be separated into segments of the time response. The commonly accepted opinion is that it is difficult to formulate a reasonable mathematical model and solution for the general time domain algorithm that includes residuals [41]. Therefore, the discussion of residuals contained in this paper will concentrate solely on the frequency domain.

Residuals and their effects have been viewed in a variety of ways, which has led to a variety of approaches to model them and applications that consider them. Residuals have been described as "asymptotic representations of other modes" and as "correction" or "compensation" terms. Some have suggested reducing computational modes with residuals, while others have suggested compensating for residuals with out-of-band modes. There are a few prevalent residual models: physical models that express residuals as the low- and high-frequency behavior of an s.d.o.f. FRF, mathematical models that represent residuals with a frequency domain power polynomial, pseudo-modes of some variant and estimation out-of-band modes.

The physical residual model is based on the asymptotic behavior in the frequency range of interest of an out-of-band, single-degree-of-freedom mode. Historically, the lower residual is a $1/\omega^2$ term and the upper residual is a constant term. This is equivalent to setting $R_l(\omega)$ to $R_{-2}\omega^{-2}$ and $R_u(\omega)$ to R_0 in Eqs. (5) and (6). The lower residual, which represents the inertia of the lower modes, is also known as inertia restraint, inertia constraint and residual inertia. The upper residual, which represents the flexibility of the upper modes, is also known as residual flexibility and residual compliance. These typical forms of the physical residuals have always been used with the implicit assumption that the out-of-band modes are "well-separated" from the in-band modes. The limits of this assumption have been established by examining the relative error between the asymptotes of an s.d.o.f. FRF and the constant and $1/\omega^2$ residuals. The residual modes must be separated from the frequency range of interest by a factor of 10 for a one-per cent agreement [42]. This is typically not the case, especially when processing a narrow sub-band of frequency; the residual modes are usually just outside of the band. If the out-of-band modes are not sufficiently separated from the in-band modes, their effects cannot be adequately described by the simple, physical residual model. Typically, the closer the out-of-band modes are to the frequency range of interest, the greater the number of residual terms that are needed to fully account for their influence.

While the residual inertia and residual flexibility terms are based on a simplification of physical frequency response characteristics, "the residual effects of modes below and/or above the frequency range of interest cannot be completely represented by such simple relationships [41]". To overcome the limitations of the single-term, physical residuals, the upper and lower residual have also been modelled with multiple-term, purely mathematical expressions, which "can have any mathematical form that is convenient as long as the lack of physical significance is understood. Power functions of frequency … are commonly used with such a limitation [43]". It is

these frequency domain power polynomials that are the basis of the generalized residual model presented in this paper.

3. Rational fraction polynomial model with generalized residuals

If the out-of-band modes are not sufficiently separated from the in-band modes, the single-term, physical residual model is not adequate to describe the residual effects in the frequency range of interest. As was mentioned above, mathematical models of power polynomials of frequency have been used to represent residuals. To better model the asymptotic behavior of the residual modes, more polynomial terms can be used of the form $\sum_k (\mathrm{j}\omega)^k R_k$, with both positive and negative orders. Since the $1/\omega^2$ term models the lower residuals, it is natural to use negative polynomial orders for the lower residual and similarly to use positive polynomial orders for the upper residual. (Although zero is not strictly either positive or negative, the zeroth order polynomial term is included in the upper residuals, with positive orders, as a notational convenience and because the constant term is the upper physical residual.) In fact, it has been shown that a polynomial function can be fit to any segment of an FRF, or a superposition of FRFs, except at the resonance peaks [42]. That is, this residual polynomial can adequately represent the asymptotic behavior of residual modes. Together the modal model and the residual model account for all of the contributions to the FRF in the frequency band.

The power polynomial residual model is incorporated into the rational fraction polynomial FRF model of Eq. (6) by letting the lower residual function $R_l(\omega)$ be a complete[1] polynomial with negative orders and the upper residual function $R_u(\omega)$ be a complete polynomial with positive orders, that is,

$$R_l(\omega) = \sum_{k=n_l}^{-1} (\mathrm{j}\omega)^k [R_{l,k}], \quad \text{where } n_l < 0 \text{ is the lower index limit of the residual polynomial,}$$

$$R_u(\omega) = \sum_{k=0}^{n_u} (\mathrm{j}\omega)^k [R_{u,k}], \quad \text{where } n_u \geqslant 0 \text{ is the upper index limit of the residual polynomial.} \tag{7}$$

Substituting these expressions for the residual functions into Eq. (6),

$$[H(\omega)] = \sum_{k=n_l}^{-1} (\mathrm{j}\omega)^k [R_{l,k}] + \frac{\sum_{k=0}^{m-2} (\mathrm{j}\omega)^k [\beta_k]}{\sum_{k=0}^{m} (\mathrm{j}\omega)^k [\alpha_k]} + \sum_{k=0}^{n_u} (\mathrm{j}\omega)^k [R_{u,k}], \tag{8}$$

and combining the upper and lower residual functions into a generalized residual polynomial that includes both the upper and lower residuals,

$$[H(\omega)] = \frac{\sum_{k=0}^{m-2} (\mathrm{j}\omega)^k [\beta_k]}{\sum_{k=0}^{m} (\mathrm{j}\omega)^k [\alpha_k]} + \sum_{k=n_l}^{n_u} (\mathrm{j}\omega)^k [R_k]. \tag{9}$$

[1] By a complete polynomial, it is meant that the integer orders of the polynomial are continuous and inclusive, that is, from a minimum order to a maximum order including all orders between.

The first term in Eq. (9) is the rational fraction polynomial modal model and the second term is the generalized residual polynomial model. Multiplying the second term by a fractional identity to create a common denominator,

$$[H(\omega)] = \frac{\sum_{k=0}^{m-2} (\mathrm{j}\omega)^k[\beta_k]}{\sum_{k=0}^{m} (\mathrm{j}\omega)^k[\alpha_k]} + \frac{\sum_{k=0}^{m} (\mathrm{j}\omega)^k[\alpha_k] \sum_{k=n_l}^{n_u} (\mathrm{j}\omega)^k[R_k]}{\sum_{k=0}^{m} (\mathrm{j}\omega)^k[\alpha_k]}. \tag{10}$$

The product of the polynomials in the numerator of the second term creates another polynomial. The coefficients of the new polynomial ($\hat{R}_k$) are linear combinations of the coefficients of the multiplied polynomials (α_k, R_k) and the indices of the new series are the sum of the indices of the multiplied series:

$$[H(\omega)] = \frac{\sum_{k=0}^{m-2} (\mathrm{j}\omega)^k[\beta_k]}{\sum_{k=0}^{m} (\mathrm{j}\omega)^k[\alpha_k]} + \frac{\sum_{k=n_l}^{m+n_u} (\mathrm{j}\omega)^k[\hat{R}_k]}{\sum_{k=0}^{m} (\mathrm{j}\omega)^k[\alpha_k]}. \tag{11}$$

The range of the indices on the numerator series of the second term in Eq. (11) is $k = n_l$ to $m + n_u$, which encompasses the range of the indices on the numerator series of the first term, $k = 0$ to $m - 2$. Combining these two numerator polynomials over the common denominator creates another numerator polynomial in which the $\hat{\beta}_k$ coefficients are a linear combination of the β_k and $\hat{R}_k$ coefficients,

$$[H(\omega)] = \frac{\sum_{k=n_l}^{m+n_u} (\mathrm{j}\omega)^k[\hat{\beta}_k]}{\sum_{k=0}^{m} (\mathrm{j}\omega)^k[\alpha_k]}, \tag{12}$$

to give the final form of the rational fraction polynomial model with generalized residuals. (Note that by allowing n_l to be 0 and n_u to be -2, residuals are effectively eliminated from the general form of Eq. (12), which reduces to the form of the rational fraction polynomial model without residuals in Eq. (2).) This generalized frequency domain power polynomial residual model is a purely mathematical construct. It does not have direct physical significance to the FRF model, but can more completely describe the contributions of the residual modes that are not well separated from the frequency range of interest.

The result is essentially a change of the numerator polynomial order indices from $k = 0, \ldots, m - 2$ to $k = n_l, \ldots, m + n_u$. However, specifying the minimum and maximum of the orders indices, n_l and n_u, for the residual polynomial in Eq. (9) is not the same as specifying the orders of the numerator polynomial in Eq. (12). The convolution of the residual polynomial with the denominator polynomial determines the orders of the numerator polynomial. The residual model is defined as a complete polynomial, and not as a spaced sequence of orders, because any omitted orders will typically be produced by the convolution with the rational fraction polynomial denominator. The residuals included in the rational fraction polynomial model are defined by specifying the values of n_l and n_u.

The numerator coefficients ($\hat{\beta}_k$) in Eq. (12) are combinations of the original numerator polynomial coefficients (β_k), the denominator polynomial coefficients (α_k) and the generalized residual polynomial coefficients (R_k) in Eq. (9). Consider the following example with $n_l = -2$, $n_u = 0$ and $m = 4$ in Eq. (9), replacing the variable $\mathrm{j}\omega$ with s and omitting the matrix notation for brevity:

$$H(s) = \frac{\beta_0 + \beta_1 s + \beta_2 s^2}{\alpha_0 + \alpha_1 s + \alpha_2 s^2 + \alpha_3 s^3 + \alpha_4 s^4} + R_{-2} s^{-2} + R_{-1} s^{-1} + R_0,$$

$$H(s) = \frac{\begin{array}{l}\alpha_0 R_{-2} s^{-2} + (\alpha_1 R_{-2} + \alpha_0 R_{-1}) s^{-1} + (\alpha_2 R_{-2} + \alpha_1 R_{-1} + \alpha_0 R_0 + \beta_0) s^0 \\ +(\alpha_3 R_{-2} + \alpha_2 R_{-1} + \alpha_1 R_0 + \beta_1) s + (\alpha_4 R_{-2} + \alpha_3 R_{-1} + \alpha_2 R_0 + \beta_2) s^2 \\ +(\alpha_4 R_{-1} + \alpha_3 R_0) s^3 + \alpha_4 R_0 s^4\end{array}}{\alpha_0 + \alpha_1 s + \alpha_2 s^2 + \alpha_3 s^3 + \alpha_4 s^4},$$

$$H(s) = \frac{\hat{\beta}_{-2} s^{-2} + \hat{\beta}_{-1} s^{-1} + \hat{\beta}_0 + \hat{\beta}_1 s + \hat{\beta}_2 s^2 + \hat{\beta}_3 s^3 + \hat{\beta}_4 s^4}{\alpha_0 + \alpha_1 s + \alpha_2 s^2 + \alpha_3 s^3 + \alpha_4 s^4}. \tag{13}$$

The $\hat{\beta}_k$ and α_k coefficients are estimated from the solution of the frequency domain Unified Matrix Polynomial Approach (UMPA) model. The β_k and R_k coefficients can be deconvolved by setting equal the like terms in the second and third lines of Eq. (13) and arranging into a matrix equation:

$$\begin{bmatrix} \alpha_0 & 0 & 0 & 0 & 0 & 0 \\ \alpha_1 & \alpha_0 & 0 & 0 & 0 & 0 \\ \alpha_2 & \alpha_1 & \alpha_0 & I & 0 & 0 \\ \alpha_3 & \alpha_2 & \alpha_1 & 0 & I & 0 \\ \alpha_4 & \alpha_3 & \alpha_2 & 0 & 0 & I \\ 0 & \alpha_4 & \alpha_3 & 0 & 0 & 0 \\ 0 & 0 & \alpha_4 & 0 & 0 & 0 \end{bmatrix} \begin{Bmatrix} R_{-2} \\ R_{-1} \\ R_0 \\ \beta_0 \\ \beta_1 \\ \beta_2 \end{Bmatrix} = \begin{Bmatrix} \hat{\beta}_{-2} \\ \hat{\beta}_{-1} \\ \hat{\beta}_0 \\ \hat{\beta}_1 \\ \hat{\beta}_2 \\ \hat{\beta}_3 \\ \hat{\beta}_4 \end{Bmatrix}. \tag{14}$$

Note that Eq. (14) has seven equations, but only six unknown β_k and R_k coefficients. A linear system of equations with more equations than unknowns has no solution unless there are redundant equations, but there are no redundant equations in Eq. (14). This condition can be rectified by recalling that the general expansion of a partial fraction model to a rational fraction polynomial model is

$$\sum_{r=1}^{m} \frac{A_r}{s - \lambda_r} = \frac{\sum_{k=0}^{m-1} \beta_k s^k}{\sum_{k=0}^{m} \alpha_k s^k}, \quad \text{where } \beta_{m-1} = \sum_{r=1}^{m} A_r. \tag{15}$$

The α_k coefficients are combinations of the poles (λ_r) and the β_k coefficients are combinations of the poles and residues (A_r), except β_{m-1}, which is equal to the summation of the residues. If the assumption is made that the system described by the partial fraction model in Eq. (15) is causal, which is a standard assumption for the modal model, the β_{m-1} term becomes zero. This is the reason that the numerator polynomial in Eqs. (2) and (8) are defined with a maximum order of $m-2$. If the $m-1$ term is included Eq. (14), then there are as many unknowns as equations and

the system of equations has a solution.

$$\begin{bmatrix} \alpha_0 & 0 & 0 & 0 & 0 & 0 & 0 \\ \alpha_1 & \alpha_0 & 0 & 0 & 0 & 0 & 0 \\ \alpha_2 & \alpha_1 & \alpha_0 & I & 0 & 0 & 0 \\ \alpha_3 & \alpha_2 & \alpha_1 & 0 & I & 0 & 0 \\ \alpha_4 & \alpha_3 & \alpha_2 & 0 & 0 & I & 0 \\ 0 & \alpha_4 & \alpha_3 & 0 & 0 & 0 & I \\ 0 & 0 & \alpha_4 & 0 & 0 & 0 & 0 \end{bmatrix} \begin{Bmatrix} R_{-2} \\ R_{-1} \\ R_0 \\ \beta_0 \\ \beta_1 \\ \beta_2 \\ \beta_3 \end{Bmatrix} = \begin{Bmatrix} \hat{\beta}_{-2} \\ \hat{\beta}_{-1} \\ \hat{\beta}_0 \\ \hat{\beta}_1 \\ \hat{\beta}_2 \\ \hat{\beta}_3 \\ \hat{\beta}_4 \end{Bmatrix}. \tag{16}$$

The β_3 coefficient computed from Eq. (16) should be zero, or nearly zero relative to the other coefficients, if the assumptions on the FRF model are correct, which could be used as a numerical check on the UMPA model solution. Another reason that generalized residuals is conceptually defined as a complete polynomial is that if any of the R_k coefficients are omitted, Eq. (16) would not have a solution.

The matrix equation in Eq. (16) is for the example above. The general form of the matrix equation to solve for the coefficients of the residual and original numerator polynomials can be determined by inspection. The first $n_u - n_l + 1$ columns are filled with a cyclic permutation of the denominator α_k coefficients and the rows corresponding to the $\hat{\beta}_0, \hat{\beta}_1, \ldots, \hat{\beta}_{m-1}$ coefficients in the last m columns are filled with an identity matrix. The original β_k coefficients are needed to determine the residues directly from the UMPA model solution, as will be used in the algorithm developed in Section 5.

4. Frequency domain UMPA model with generalized residuals

The frequency domain UMPA model can be derived by rearranging the rational fraction polynomial MIMO FRF model in Eq. (2) as

$$\sum_{k=0}^{\bar{m}} [(\mathrm{j}\omega)^k[\alpha_k]][H(\omega)] = \sum_{k=0}^{\bar{m}-2} (\mathrm{j}\omega)^k[\beta_k]. \tag{17}$$

The frequency domain UMPA model that includes generalized residuals can be derived by rearranging Eq. (12) as

$$\sum_{k=0}^{m} [(\mathrm{j}\omega)^k[\alpha_k]][H(\omega)] = \sum_{k=n_l}^{m+n_u} (\mathrm{j}\omega)^k[\hat{\beta}_k]. \tag{18}$$

By letting $[\alpha_m]$ be an identity matrix and rearranging, the linear matrix equation is

$$\sum_{k=0}^{m-1} [(\mathrm{j}\omega)^k[\alpha_k]][H(\omega)] - \sum_{k=n_l}^{m+n_u} (\mathrm{j}\omega)^k[\hat{\beta}_k] = -(\mathrm{j}\omega)^m[H(\omega)] \tag{19}$$

or in matrix form

$$[[\alpha_0][\alpha_1]\cdots[\alpha_{m-1}][\hat{\beta}_{n_l}]\cdots[\hat{\beta}_{m+n_u}]]\begin{bmatrix}[H(\omega)]\\ \mathrm{j}\omega[H(\omega)]\\ \vdots\\ (\mathrm{j}\omega)^{m-1}[H(\omega)]\\ -(\mathrm{j}\omega)^{n_l}[I]\\ \vdots\\ -(\mathrm{j}\omega)^{m+n_u}[I]\end{bmatrix} = -(\mathrm{j}\omega)^m[H(\omega)]. \tag{20}$$

Note that the only difference between the UMPA models in Eqs. (17) and (18) is the range of the indices on the right-hand side polynomial series. Thus, all of the developments related to the basic UMPA model are also valid for the UMPA model that includes generalized residuals in Eq. (18).

5. An s.d.o.f. frequency domain algorithm with generalized residuals

One application of the UMPA model with generalized residuals is in the area of single-degree-of-freedom algorithms. When only one mode is of interest, but the other modes are not well-separated (i.e., by a factor of 10), the traditional s.d.o.f. methods (e.g., Co/Quad, finite difference, least-square local, least-squares global, etc.) do not adequately represent the FRF characteristics due to the lack of residuals in their formulation. Increasing the model order to account for other modes produces additional computational poles that must be sorted to identify the actual pole of interest. A preferred alternative would be to only calculate the single desired pole and use residuals to account for all nearby modes. This new method includes generalized residuals and is formulated as a global, low order, frequency domain, short basis, single-input/multiple-output (SIMO) algorithm. Additionally, the residues can be calculated directly from the UMPA model solution by deconvolving the resulting $\lfloor \beta_k \rfloor$ and $\lfloor R_k \rfloor$ vectors, as shown above. (While the inclusion of negative powers of ω in the residual polynomial does create a singularity at $\omega = 0$, this is not a practical issue because $\omega = 0$ is never included in the frequency band used to identify the system poles.)

The partial fraction model of Eq. (21) and the rational fraction polynomial model of Eq. (22) both represent the frequency response matrix of a system:

$$[H(\omega)] = \sum_{r=1}^{2N} \frac{[A_r]}{\mathrm{j}\omega - \lambda_r}, \tag{21}$$

$$[H(\omega)] = \frac{\sum_{k=0}^{m-2} (\mathrm{j}\omega)^k[\beta_k]}{\sum_{k=0}^{m} (\mathrm{j}\omega)^k[\alpha_k]}, \quad \text{where } m \geqslant 2. \tag{22}$$

FRFs can be synthesized by Eq. (21) with the estimated poles and residues, but FRFs can also be synthesized by Eq. (22) with the $[\alpha_k]$ and $[\beta_k]$ polynomial coefficients from the UMPA model solution. Since the rational fraction polynomials can synthesize an FRF that replicates both its

resonance and magnitude characteristics, it stands to reason that the residue information must also be contained in the $[\beta_k]$ polynomial.

To reveal the relationship between the residues and $[\beta_k]$ polynomial, consider a single-input/single-output (SISO), s.d.o.f. system and expand the partial fraction model as

$$H(\omega) = \frac{A_1}{j\omega - \lambda_1} + \frac{A_2}{j\omega - \lambda_2}, \quad H(\omega) = \frac{(j\omega - \lambda_2)A_1 + (j\omega - \lambda_1)A_2}{(j\omega - \lambda_1)(j\omega - \lambda_2)},$$

$$H(\omega) = \frac{j\omega(A_1 + A_2) - \lambda_2 A_1 - \lambda_1 A_2}{(j\omega)^2 - j\omega(\lambda_1 + \lambda_2) + \lambda_1\lambda_2}, \quad H(\omega) = \frac{j\omega\beta_1 + \beta_0}{(j\omega)^2\alpha_2 + j\omega\alpha_1 + \alpha_0}, \tag{23}$$

which is now in the form of a rational fraction polynomial model. By equating the like terms in the third and fourth lines of Eq. (23), with $\beta_1 = 0$, and arranging into a matrix equation, the residues can be computed as

$$\begin{bmatrix} 1 & 1 \\ -\lambda_2 & -\lambda_1 \end{bmatrix} \begin{Bmatrix} A_1 \\ A_2 \end{Bmatrix} = \begin{Bmatrix} 0 \\ \beta_0 \end{Bmatrix}. \tag{24}$$

Eq. (24) can be further simplified by using the relations

$$\lambda_1 = \sigma_1 + j\omega_1, \quad \lambda_2 = \lambda_1^* = \sigma_1 - j\omega_1 \quad \text{and} \quad A_2 = -A_1, \tag{25}$$

which gives the direct solution of the residue (A_1) of a SISO, s.d.o.f. system from the β_0 coefficient of the UMPA model numerator polynomial as

$$A_1 = \frac{\beta_0}{2j\omega_1}. \tag{26}$$

This procedure can be extended to a SISO m.d.o.f. system, and also, under certain conditions, to a MIMO m.d.o.f. system [42]. For a SIMO s.d.o.f. system, as in the parameter estimation algorithm developed here, Eq. (20) can be simplified as follows:

$$[\alpha_0 \alpha_1 \lfloor \hat{\beta}_{n_l} \rfloor \cdots \lfloor \hat{\beta}_{2+n_u} \rfloor] \begin{bmatrix} \lfloor H(\omega) \rfloor \\ (j\omega)\lfloor H(\omega) \rfloor \\ -(j\omega)^{n_l}[I] \\ \vdots \\ -(j\omega)^{2+n_u}[I] \end{bmatrix} = -(j\omega)^2 \lfloor H(\omega) \rfloor, \tag{27}$$

where the row vectors, $\lfloor \hat{\beta}_k \rfloor$ and $\lfloor H(\omega) \rfloor$, are of size $(1 \times N_o)$.

By loading the matrices appropriately and including the conjugate frequencies ($H(-\omega)$) in the set of equations generated from Eq. (27), the solution vector, $[\alpha_0\, \alpha_1 \lfloor \hat{\beta}_{n_l} \rfloor \cdots \lfloor \hat{\beta}_{2+n_u} \rfloor]$, will be strictly real. Combining the solution of Eq. (27) with a generalization of Eq. (16) allows the

extraction of the underlying vector of $\lfloor \beta_0 \rfloor$ coefficients, with one β_0 coefficient for each output d.o.f.

$$\begin{bmatrix} \alpha_0 & 0 & \cdots & \cdots & 0 & 0 & 0 \\ \alpha_1 & \ddots & \ddots & & \vdots & \vdots & \vdots \\ 1 & \ddots & \ddots & \ddots & \vdots & 1 & 0 \\ 0 & \ddots & \ddots & \ddots & 0 & 0 & 1 \\ \vdots & \ddots & \ddots & \ddots & \alpha_0 & 0 & 0 \\ \vdots & & \ddots & \ddots & \alpha_1 & \vdots & \vdots \\ 0 & \cdots & \cdots & 0 & 1 & 0 & 0 \end{bmatrix} \begin{Bmatrix} \lfloor R_{n_l} \rfloor \\ \vdots \\ \vdots \\ \vdots \\ \lfloor R_{n_u} \rfloor \\ \lfloor \beta_0 \rfloor \\ \lfloor \beta_1 \rfloor \end{Bmatrix} = \begin{Bmatrix} \lfloor \hat{\beta}_{n_l} \rfloor \\ \vdots \\ \lfloor \hat{\beta}_0 \rfloor \\ \lfloor \hat{\beta}_1 \rfloor \\ \vdots \\ \vdots \\ \lfloor \hat{\beta}_{2+n_u} \rfloor \end{Bmatrix}. \tag{28}$$

Solving for the roots (λ_1 and λ_2) of the characteristic equation, $s^2 + \alpha_1 s + \alpha_0 = 0$, and combining with Eq. (26) provides the final form of the solution, the simultaneous solution for a single global pole and a vector of residues:

$$\lfloor A_1 \rfloor = \frac{\lfloor \beta_0 \rfloor}{2j\omega_1}. \tag{29}$$

Therefore, the final SIMO modal parameters are λ_1 and $\lfloor A_1 \rfloor$.

5.1. Three d.o.f. analytical example

To demonstrate the effectiveness of this technique, a 3-d.o.f. example is introduced, and then the modal parameters of the second mode are estimated with the s.d.o.f. frequency domain algorithm for several residual polynomials. The FRF synthesized from the estimated α_k and $\hat{\beta}_k$ coefficients is compared to the analytical function in Fig. 2 for no residuals (i.e., $n_l = 0$ and $n_u = -2$), in Fig. 3 for the physical residuals (i.e., $n_l = -2$ and $n_u = 0$) and in Fig. 5 for a general residual polynomial ($n_l = -4$ and $n_u = 4$). The magnitudes of the residual polynomial coefficients are also plotted in Figs. 4 and 6. The inset plot in Figs. 2, 3 and 5 details the comparison of the analytical and synthesized functions in the region near the resonance peak. In Fig. 7, the FRF is synthesized from Eq. (17) using the coefficients of the original numerator polynomial without residuals (β_0) and of the residual polynomial ($R_{-4}, \ldots, R_4$), which were determined from Eq. (28). This plot is included to show that the same FRF is synthesized from Eqs. (17) and (18) and to verify the deconvolution of the estimated numerator polynomial into the original numerator and residual polynomials. In Fig. 8, the residual polynomial is synthesized and compared to the function synthesized using only modes 1 and 3 to illustrate that the residual polynomial does indeed account for the residual contributions of modes 1 and 3 in the frequency range of interest. The estimated modal parameters are listed in Table 1.

The plots in Figs. 2–8 and the results in Table 1 show that the greatest error in the estimated modal parameters is for the case with no residuals and the accuracy improves by including residuals in the parameter estimation model. In this case, the physical residuals were adequate to compensate for the out-of-band modes, but this system had relatively well-spaced modes.

The next system has more closely spaced modes and again the modal parameters of the second mode are estimated with the s.d.o.f. frequency domain algorithm for several residual polynomials.

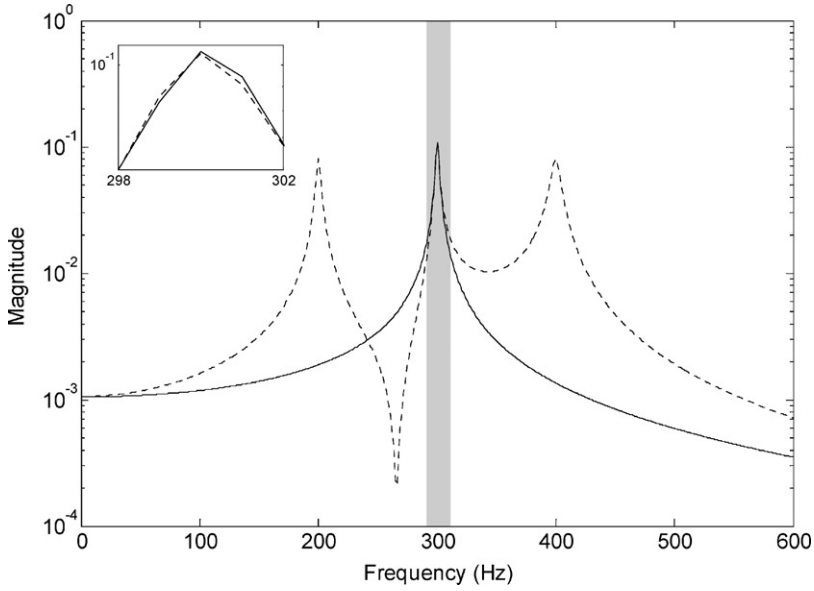

Fig. 2. Comparison of a 3-d.o.f. analytical FRF (dashed line) and the FRF synthesized from the estimated polynomial coefficients (solid line), with no residuals.

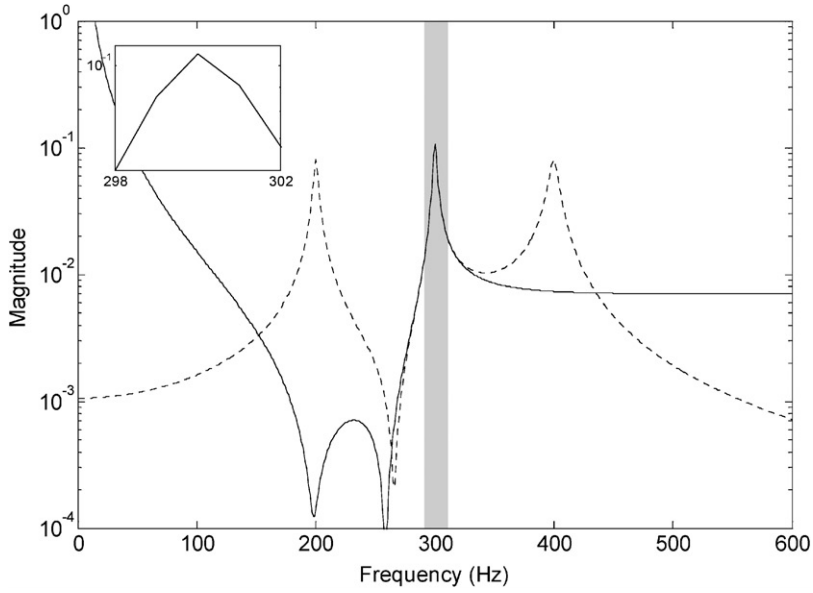

Fig. 3. Comparison of a 3-d.o.f. analytical FRF (dashed line) and the FRF synthesized from the estimated polynomial coefficients (solid line), with physical residuals.

The FRF synthesized from the estimated α_k and $\hat{\beta}_k$ coefficients is compared to the analytical function in Fig. 9 for no residuals, in Fig. 10 for the physical residuals and in Fig. 12 for a general residual polynomial ($n_l = -12$ and $n_u = 12$). The magnitudes of the residual polynomial

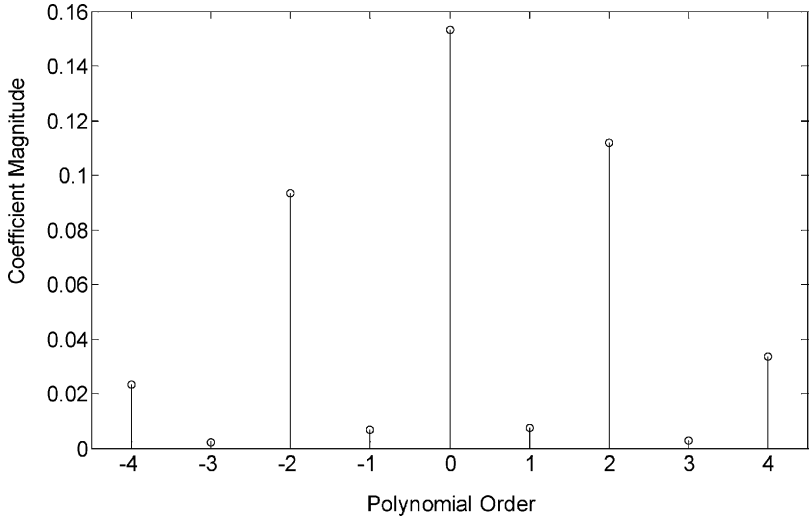

Fig. 4. Magnitude of residual polynomial coefficients for Fig. 3.

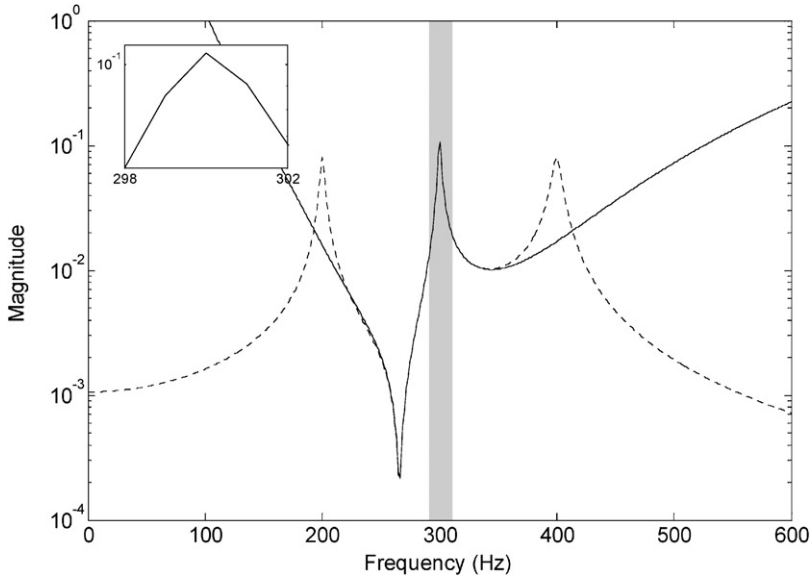

Fig. 5. Comparison of a 3-d.o.f. analytical FRF (dashed line) and the FRF synthesized from the estimated polynomial coefficients (solid line), with a generalized residual polynomial of orders $-4 : 4$.

coefficients are also plotted in Figs. 11 and 13. The inset plot in Figs. 9, 10 and 12 details the comparison of the original and synthesized functions in the region near the resonance peak. The estimated modal parameters are listed in Table 2.

The plots in Figs. 9–13 and the results in Table 2 show essentially the same results as the preceding example in that the greatest error in the estimated modal parameters is for the case with

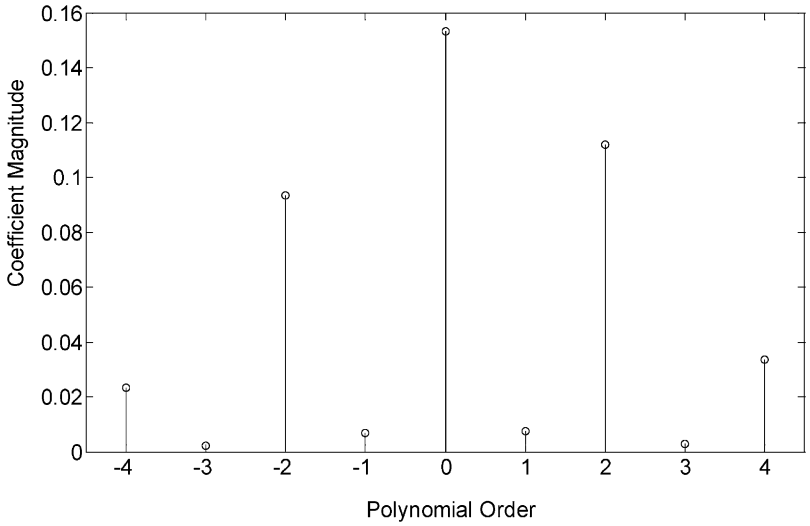

Fig. 6. Magnitude of residual polynomial coefficients for Fig. 5.

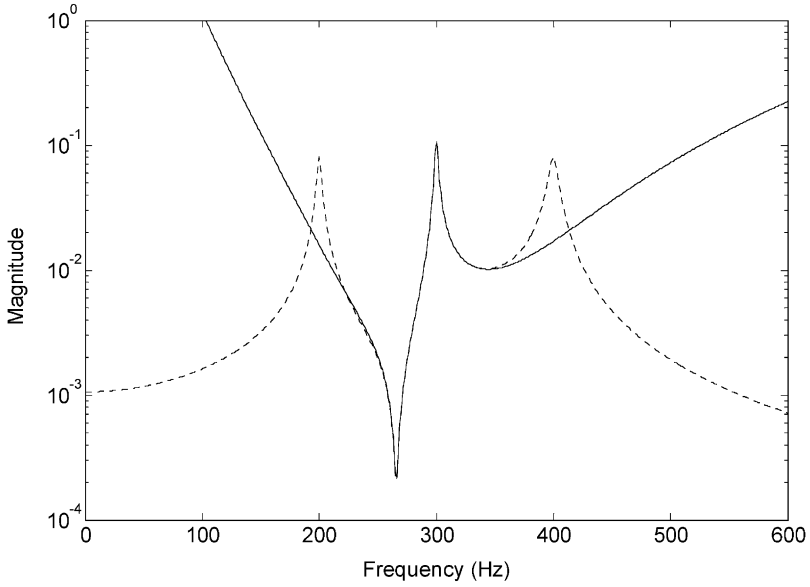

Fig. 7. Comparison of a 3-d.o.f. analytical FRF (dashed line) and the FRF synthesized from the estimated and deconvolved polynomial coefficients (solid line), with a generalized residual polynomial of orders $-4 : 4$.

no residuals and the accuracy improves by including residuals in the parameter estimation model. However, there is much greater error with no residuals and still some error with the physical residuals. In this case, a generalized residual polynomial with more orders was needed to accurately estimate the modal parameters. This is typical, that is, the closer the out-of-band modes are to the frequency range of interest, the more residual terms that are required to completely

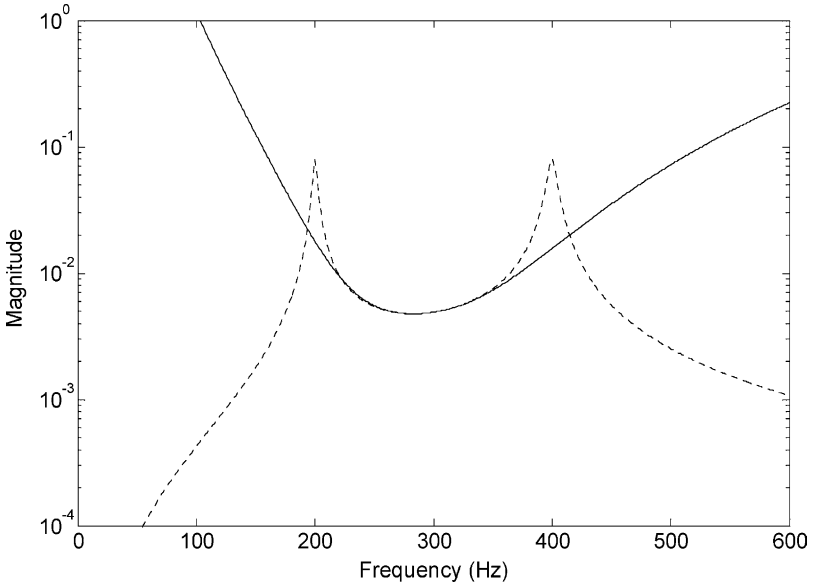

Fig. 8. Comparison of the generalized residual polynomial with orders $-4:4$ to the contribution of the residual modes.

Table 1
Estimated modal parameters of 3-d.o.f. system with well-separated modes

Residuals	Frequency (Hz)	Frequency error (Hz)	Damping (%)	Damping error (%)	Residue	Residue error
Analytical system	300		0.5		$0-j1.00$	
$n_l=0, n_u=-2$ (no residuals)	300.2048	$+0.2048$	0.4880	-0.012	$0.0000-j0.9931$	$+0.0000+j0.0069$
$n_l=-2, n_u=0$	300.0008	$+0.0008$	0.5000	0	$0.0000-j1.0000$	0
$n_l=-4, n_u=4$	300.0000	0	0.5000	0	$0.0000-j1.0000$	0

account for their effects. Note however for this example, while the absolute differences appear small, it must be recognized that this is analytical data (i.e., no noise) and as such any differences are significant and therefore the last case represents an order of magnitude improvement in the fit error.

5.2. Complex mode indicator function experimental example

To demonstrate the practical application of generalized residuals, a second example which utilizes experimentally measured FRFs and the Complex Mode Indicator Function (CMIF) [44] is presented. The CMIF was originally developed as an aid to model order determination for multiple reference datasets [23], but has since become the basis for a spatial domain parameter

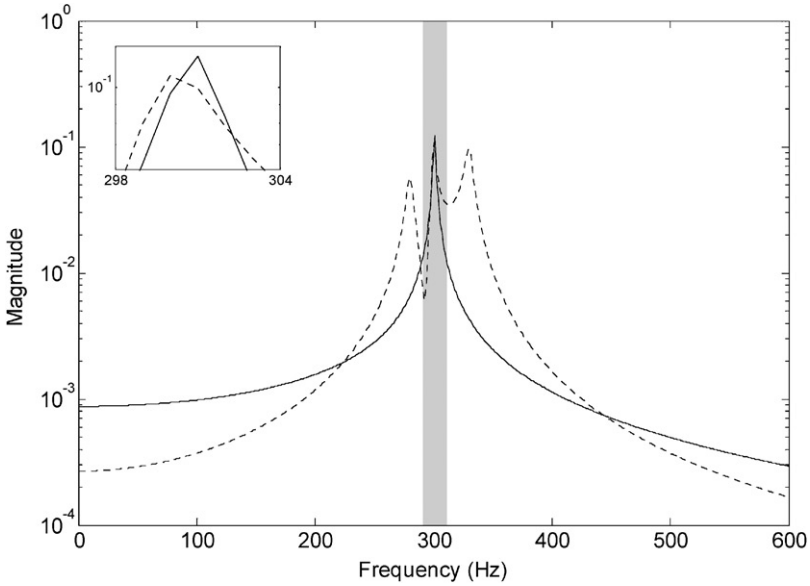

Fig. 9. Comparison of a 3-d.o.f. analytical FRF (dashed line) and the FRF synthesized from the estimated polynomial coefficients (solid line), with no residuals.

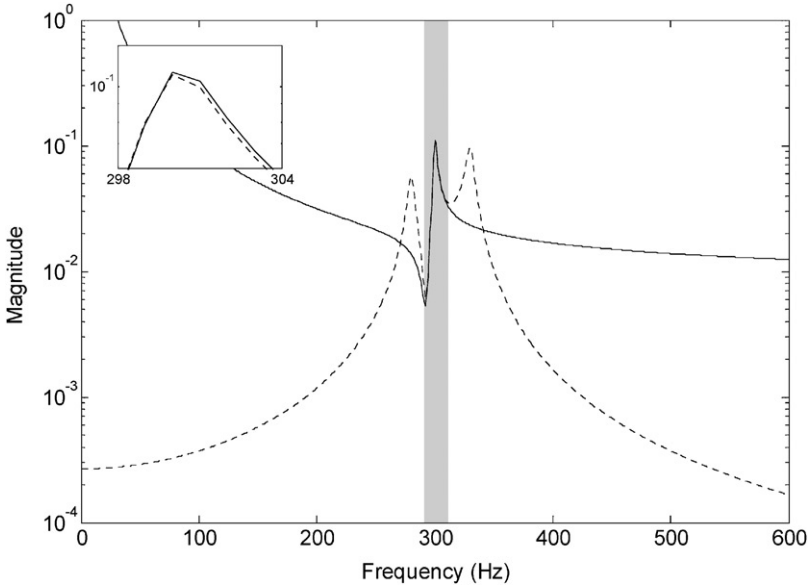

Fig. 10. Comparison of a 3-d.o.f. analytical FRF (dashed line) and the FRF synthesized from the estimated polynomial coefficients (solid line), with physical residuals.

estimation algorithm [45,46]. The common approach in modal parameter estimation is a two-stage, linear process. The majority of frequency domain algorithms, as well as time domain algorithms, produce temporal information, the poles, in the first stage, and scaled spatial

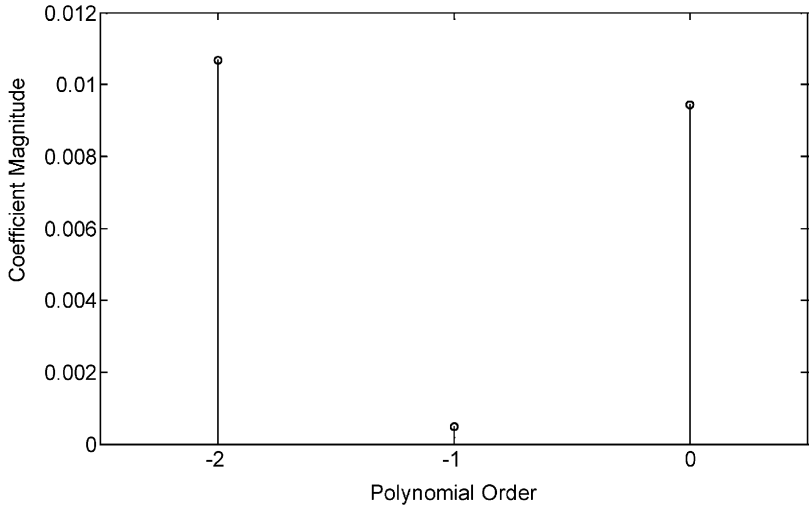

Fig. 11. Magnitude of residual polynomial coefficients for Fig. 10.

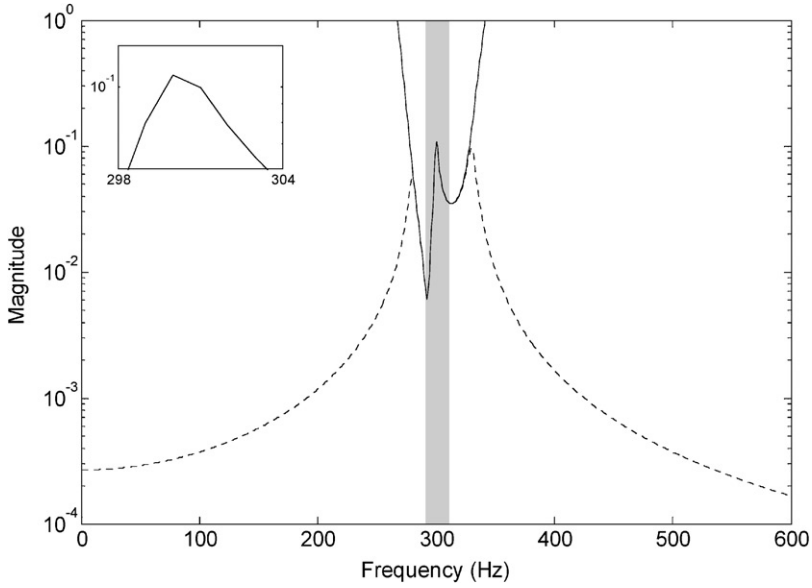

Fig. 12. Comparison of a 3-d.o.f. analytical FRF (dashed line) and the FRF synthesized from the estimated polynomial coefficients (solid line), with a generalized residual polynomial of orders $-12 : 12$.

information, the modal vectors and modal scaling, in the second stage. Conversely, spatial domain algorithms produce unscaled spatial information, the modal vectors, in the first stage and temporal and scaling information, the poles and modal scaling, in the second stage. A spatial domain algorithm is classified as a zero order UMPA model, which is an algorithm that is "programmed to process data at a single temporal condition (frequency or time) [1]".

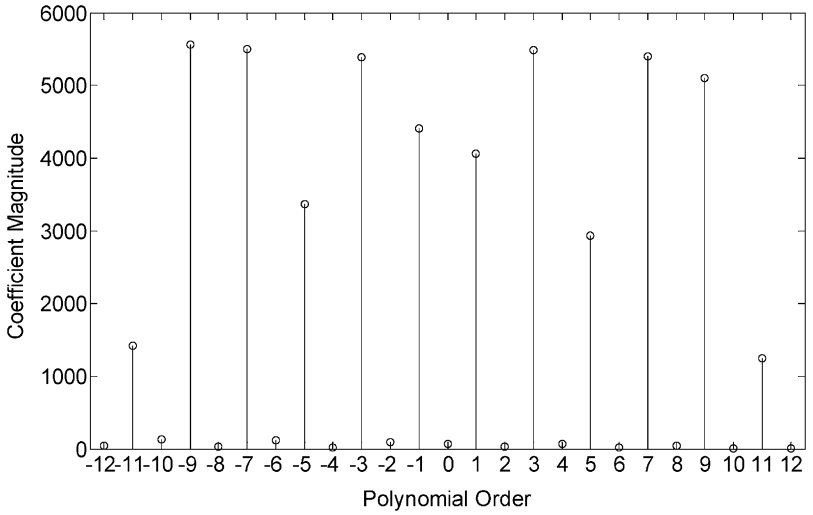

Fig. 13. Magnitude of residual polynomial coefficients for Fig. 12.

Table 2
Estimated modal parameters of 3-d.o.f. system with closely spaced modes

Residuals	Frequency (Hz)	Frequency error (Hz)	Damping (%)	Damping error (%)	Residue	Residue error
Analytical system	300		0.5		$0 - j1.00$	
$n_l = 0, n_u = -2$ (no residuals)	300.8512	$+0.8512$	0.3545		$0.0000 - j0.8265$	$+0.0000 + j0.1735$
$n_l = -2, n_u = 0$	300.0603	$+0.0603$	0.4923		$0.0000 - j0.9936$	$+0.0000 + j0.0064$
$n_l = -12, n_u = 12$	300.0000	0	0.5000	0	$0.0000 - j1.0004$	$-0.0000 - j0.0004$

The CMIF is formed by computing the economical singular-value decomposition (SVD) of the FRF matrix at each spectral line,

$$\underset{(N_o \times N_i)}{[H(\omega_k)]} = \underset{(N_o \times N_i)}{[U_k]} \quad \underset{(N_i \times N_i)}{[\Sigma_k]} \quad \underset{(N_i \times N_i)}{[V_k]^{\mathrm{H}}}, \tag{30}$$

where $[\Sigma_k]$ is a diagonal matrix of real, non-negative singular values in descending order, $[U_k]$ is the matrix of left singular vectors and $[V_k]$ is the matrix of right singular vectors, for $N_o \geqslant N_i$. If this is not the case, then the CMIF processes the transpose of the FRF matrix.

A CMIF is a plot of the singular values as a function of frequency, usually on a log-magnitude scale, with one curve for each singular value. Often the "tracked" CMIF is plotted to alleviate the singular-value crossover effect [44]. The peaks in the CMIF curves coincide with the resonances of the system and locate the damped natural frequency of the modes to the nearest spectral line. The left singular vector associated with the significant singular value at a CMIF peak is an approximation of the mode shape, and the right singular vector is an approximation of the modal

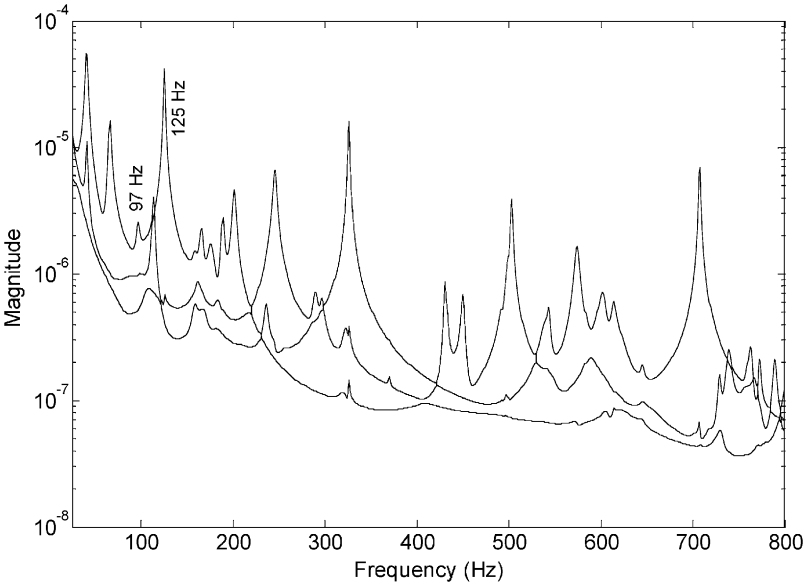

Fig. 14. Complex mode indicator function of a measured FRF dataset.

participation factors. Fig. 14 shows the CMIF of a measured dataset of FRFs for a system with $N_o = 145$, $N_i = 3$ and $\Delta f = 1$ Hz.

To use the CMIF parameter estimation method, the peaks in the CMIF curves corresponding to modes of the system are selected by the operator. This is usually a straightforward task, but in some instances additional analysis techniques, such as the Modal Assurance Criterion (MAC) [47], mode tracking [1] and consistency diagrams, are needed to select a valid set of modes. If two CMIF curves have a peak at the same, or nearly the same, frequency, then there are two significant singular vectors, which indicates a repeated, or pseudo-repeated, mode of multiplicity two. This same reasoning also applies to modes of multiplicity greater than two. The approximate modal vectors and participation factors obtained in the first stage of the CMIF method are used to generate an enhanced frequency response function (eFRF) for each mode. The poles are then estimated from the eFRFs, which must be scaled correctly [44,48] to also be used to estimate the modal scaling [46]. (In contrast, time and frequency domain algorithms utilize the poles obtained in the first stage to estimate the residues in the second stage.) The left and right singular vectors at the CMIF peaks create a spatial filter that transforms the measured FRF matrix from the physical space to the modal space and creates a virtual measurement that enhances the mode of interest. The eFRF for mode s, $eH_s(\omega_k)$, is a scalar function that is generated at each spectral line as

$$\underset{(1\times1)}{eH_s(\omega_k)} = \underset{(1\times N_o)}{\{U_s\}^{\mathrm{T}}}\ \underset{(N_o\times N_i)}{[H(\omega_k)]}\ \underset{(N_i\times1)}{\{V_k\}} = \{U_s\}^{\mathrm{T}}\left[\sum_{r=1}^{2N}\frac{\{\Psi_r\}\{L_r\}^{\mathrm{T}}}{\mathrm{j}\omega-\lambda_r}\right]\{V_s\}. \tag{31}$$

The effect of this operation is to attenuate the contribution of all modes except mode s, thus enhancing this mode. The degree of enhancement is dependent on the inner-product of the left

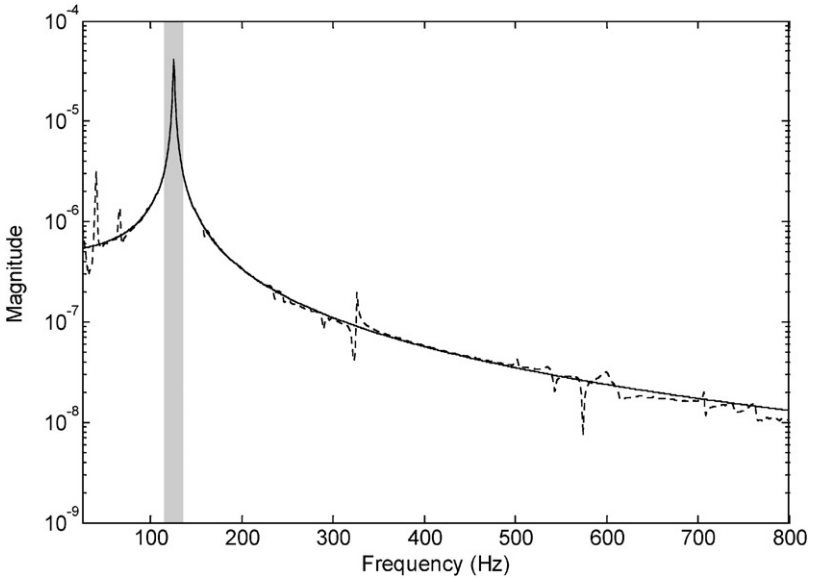

Fig. 15. Enhanced frequency response function for the mode at 125 Hz; generated from measured FRFs (dashed line) and synthesize from UMPA model (solid line).

singular vector $\{U_s\}$ and the modal vectors $\{\Psi_r\}$. If the spatial distribution of the d.o.f.s. is such that the mode shapes are sufficiently dissimilar, then the inner-product will approach zero for $r \neq s$ and mode r will not significantly contribute to the summation in Eq. (31). Ideally, the transformation uncouples the eFRF into an s.d.o.f. function in the region near the principal peak, such as in Fig. 15. Then the pole can be estimated from the eFRF for each mode with a scalar, s.d.o.f. frequency domain model:

$$[(\mathrm{j}\omega)^2\alpha_2 + (\mathrm{j}\omega)\alpha_1 + \alpha_0]eH(\omega) = \beta_0. \tag{32}$$

The eFRF generated by Eq. (31) of the CMIF peak marked at 125 Hz in Fig. 14 is plotted in Fig. 15, also plotted is the eFRF synthesized by Eq. (32) with the estimated α_k and β_0 polynomial coefficients. The shaded region indicates the frequency band around the peak evaluated in the parameter estimation algorithm. The estimated frequency was 125.270 Hz and the damping ratio was 0.595%. This example shows that if the eFRF is uncoupled into a s.d.o.f. function, at least near the principal peak, an s.d.o.f. algorithm is adequate to estimate the pole and residuals are not needed.

If the eFRF does not isolate the mode of interest, the surrounding modes will influence the estimation of pole and a simple s.d.o.f. algorithm is not sufficient. The basic idea of the CMIF parameter estimation method is to select peaks from the CMIF curves and obtain the mode shape and pole for that mode directly. Increasing the model α-order is not a preferable modification of the algorithm to account for the other modes present in the eFRF, because to do so would introduce computational poles, which is contrary to the benefits of the CMIF method. Since these other modes in the eFRF are just residuals with respect to the mode of interest, an s.d.o.f. algorithm with a generalized residual polynomial, such as that in Section 5 with the FRF replaced

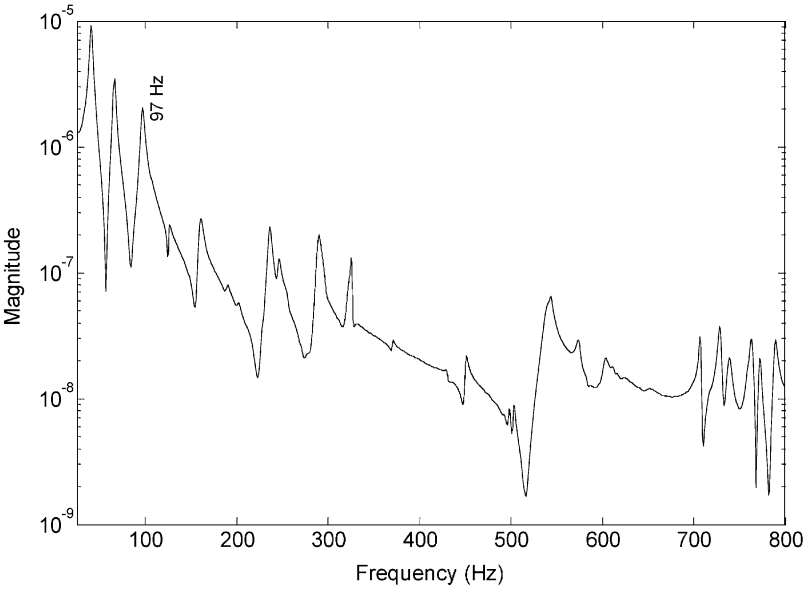

Fig. 16. Enhanced frequency response function for the mode at 97 Hz.

with an eFRF, is appropriate for the CMIF method:

$$\sum_{k=0}^{2} [(\mathrm{j}\omega)^k \alpha_k] eH(\omega) = \sum_{k=n_l}^{n_u+2} (\mathrm{j}\omega)^k \hat{\beta}_k. \tag{33}$$

The eFRF of the CMIF peak marked at 97 Hz in Fig. 14 is shown in Fig. 16. It is not an s.d.o.f. function near the principal peak, but has significant contribution of some nearby modes which were not attenuated by the spatial filter. Some residuals are needed in the parameter estimation algorithm to account for the other modes in the eFRF, but which residual polynomial? Instead of trial and error with different residual polynomials, a consistency diagram can be generated with the indices of the residual polynomial (n_l and n_u) as the variable parameters in the UMPA model. In a traditional consistency diagram for model α-order, only the value of m, the upper order of the denominator m polynomial, can be varied (e.g., $m = 2, 3, \ldots, 10$). In a consistency diagram for residuals, the values of n_l, n_u or both can be varied. The indices n_l and n_u define the orders of the generalized residual polynomial $\sum_{k=n_l}^{n_u} (\mathrm{j}\omega)^k R_k$, which multiplies with $\sum_{k=0}^{2} (\mathrm{j}\omega)^k \alpha_k$ and combines with β_0 to form the numerator polynomial of $\sum_{k=n_l}^{n_u+2} (\mathrm{j}\omega)^k \hat{\beta}_k$.

The consistency diagram for the peak at 97 Hz is shown in Fig. 17 for varying n_l, in Fig. 18 for varying n_u and in Fig. 19 for varying both n_l and n_u. Table 3 lists the orders of the residual polynomial for the model variations of the consistency diagrams in Figs. 17–19. The consistency criteria are: 1% for frequency, 5% for damping, 1% for conjugates and 10^{-6} for reciprocal of the condition number. (The meaning of the consistency diagram symbols are as follows: ○ implies that the conjugate pole exists within the specified tolerance, ∇ implies that the frequency calculated for two successive model iterations is within the specified tolerance, Δ implies that both the frequency and damping calculated for two successive model iterations is within the specified

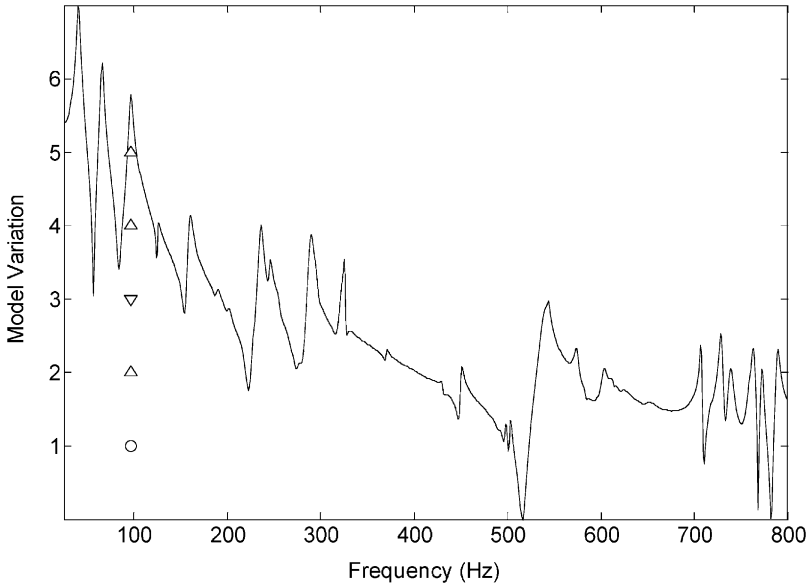

Fig. 17. CMIF method consistency diagram of the mode at 97 Hz, for varying the lower order of the residual polynomial: Δ, pole; ∇, frequency; ○, conjugate; ×, not conjugate; ∗, 1/condition.

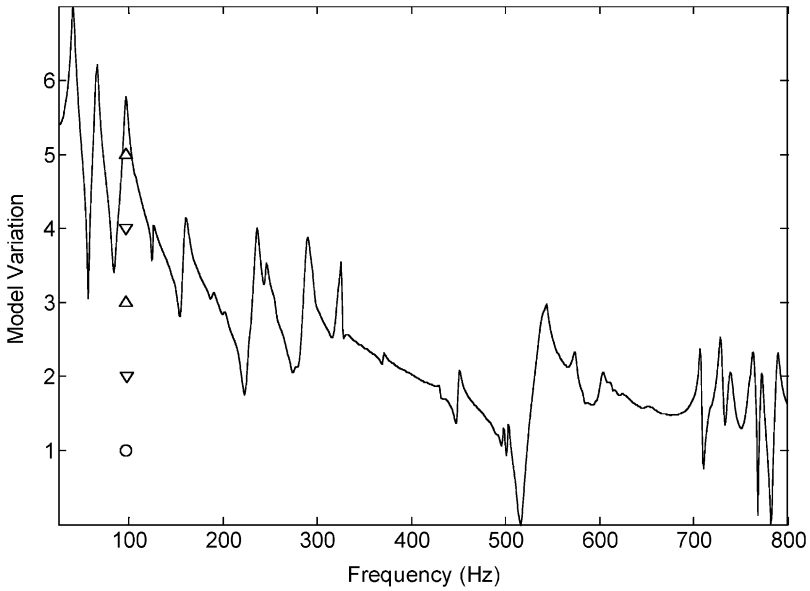

Fig. 18. CMIF method consistency diagram of the mode at 97 Hz, for varying the upper order of the residual polynomial. Δ, pole; ∇, frequency; ○, conjugate; ×, not conjugate; ∗, 1/condition.

tolerance, and ∗ implies that the numerical conditioning for that model variation solution fell below the specified tolerance.) Fig. 20 is the eFRF synthesized by Eq. (33) for all model variations of the consistency diagram in Fig. 19, the inset plot shows the region near the peak of

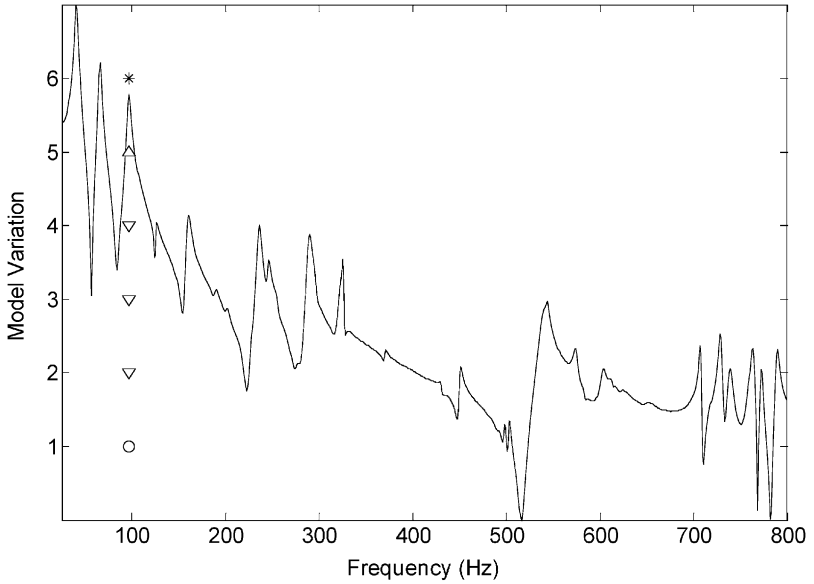

Fig. 19. CMIF method consistency diagram of the mode at 97 Hz, for varying the lower and upper orders of the residual polynomial. Δ, pole; ∇, frequency; ○, conjugate; ×, not conjugate; ∗, 1/condition.

Table 3
The lower and upper orders of the residual polynomial for the model variations of the consistency diagrams in Figs. 17– 19

	Fig. 17	Fig. 18	Fig. 19
1	$n_l = 0, n_u = -2$ (no residuals)	$n_l = 0, n_u = -2$ (no residuals)	$n_l = 0, n_u = -2$ (no residuals)
2	$n_l = 0, n_u = 1$	$n_l = -1, n_u = 0$	$n_l = 0, n_u = 0$
3	$n_l = 0, n_u = 2$	$n_l = -2, n_u = 0$	$n_l = -1, n_u = 1$
4	$n_l = 0, n_u = 3$	$n_l = -3, n_u = 0$	$n_l = -2, n_u = 2$
5	$n_l = 0, n_u = 4$	$n_l = -4, n_u = 0$	$n_l = -3, n_u = 3$
6			$n_l = -4, n_u = 4$

interest. Fig. 21 is the synthesized eFRF for model variation number 5, the first consistent pole. In Table 4 is a list of the poles estimated for the model variations of the consistency diagram in Fig. 19.

Fig. 22 is the consistency diagram for the earlier example of the mode at 125 Hz of Fig. 15, the orders of the residual polynomial and the estimated poles for the model variations are listed in Table 5. For this case of an uncoupled eFRF, the pole is consistent without residuals. However, the addition of residuals does not adversely affect the estimation of the pole, until the numerator polynomial order becomes high enough to cause poor numerical conditioning in the UMPA model solution. Table 5 is a list of the modal parameters estimated for the model variations of the consistency diagram in Fig. 22.

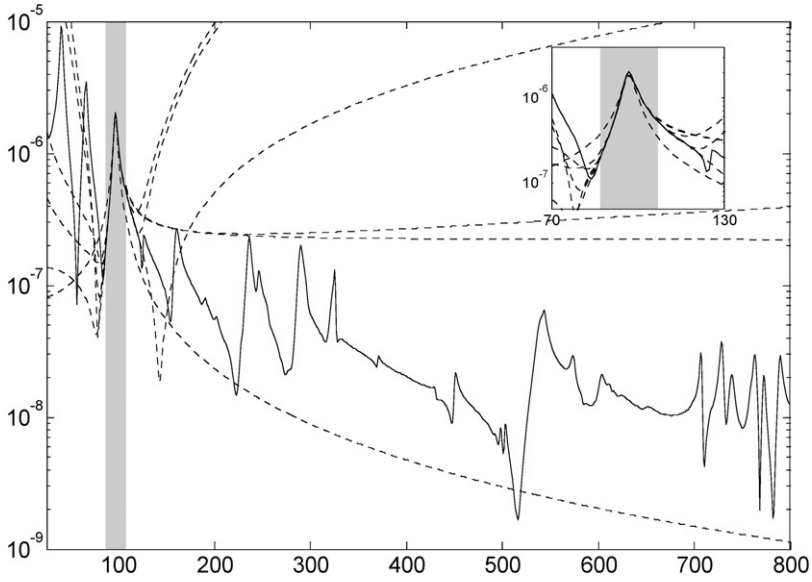

Fig. 20. Enhanced frequency response function for the mode at 97 Hz; generated from measured FRFs (solid line) and synthesized from UMPA model for all residual polynomials of the consistency diagram in Fig. 19 (dashed lines).

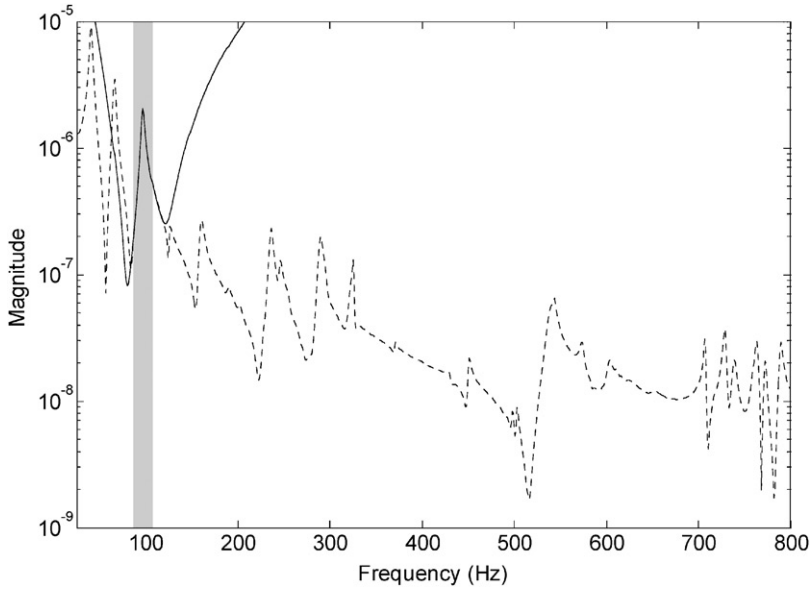

Fig. 21. Enhanced frequency response function for the mode at 97 Hz; generated from measured FRFs (solid line) and synthesized from UMPA model variation 5 in Fig. 19 (dashed lines).

6. Application considerations

The use of residuals as a consistency criterion represents an important paradigm shift for modal analysis. While many parameter estimation problems can be solved reasonably using the

Table 4
The estimated poles for the model variations of the consistency diagram in Fig. 19

	Residuals	Frequency (Hz)	Damping (%)	Consistency	1/Condition
1	$n_l = 0, n_u = -2$ (no residuals)	97.002	1.898	Conjugate	3.777e-001
2	$n_l = 0, n_u = 0$	96.895	2.190	Frequency	5.149e-002
3	$n_l = -1, n_u = 1$	96.929	1.903	Frequency	2.645e-003
4	$n_l = -2, n_u = 2$	96.900	2.058	Frequency	1.365e-003
5	$n_l = -3, n_u = 3$	96.880	2.052	Pole	6.962e-006
6	$n_l = -4, n_u = 4$	96.880	2.070	1/Condition	3.509e-007

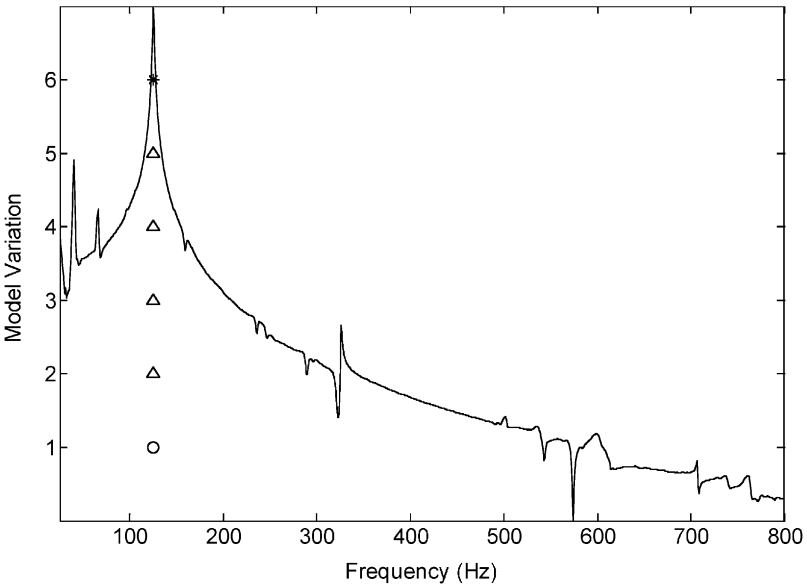

Fig. 22. CMIF method consistency diagram of the mode at 125 Hz. Δ, pole; ∇, frequency; ○, conjugate; ×, not conjugate; ∗, 1/condition.

Table 5
The lower and upper orders of the residual polynomial and the estimated poles for the model variations of the consistency diagram in Fig. 22

	Residuals	Frequency (Hz)	Damping (%)	Consistency	1/Condition
1	$n_l = 0, n_u = -2$ (no residuals)	125.270	0.595	Conjugate	3.220e-001
2	$n_l = 0, n_u = 0$	125.264	0.595	Pole	4.476e-002
3	$n_l = -1, n_u = 1$	125.263	0.592	Pole	1.826e-003
4	$n_l = -2, n_u = 2$	125.263	0.592	Pole	7.292e-005
5	$n_l = -3, n_u = 3$	125.263	0.593	Pole	2.887e-006
6	$n_l = -4, n_u = 4$	125.263	0.593	1/Condition	1.137e-007

traditional approach of varying the order of the denominator polynomial, there are many problems for which this approach is unsuccessful. One area that does not lend itself well to the traditional parameter estimation approaches involves the analysis of highly noisy, slightly inconsistent data. For this condition, each model iteration generates an entirely new set of system pole estimates with little consistent characteristic. Often, however, the number of active modes within a given frequency range may be identified using other techniques, for example the complex mode indicator function (CMIF). In this case then, it is better to fix the denominator polynomial (i.e., number of poles) and iterate over the numerator polynomial (i.e., residuals) until a consistent solution is obtained. One real world example for which this approach has been found to be highly effective is the testing of bridges [49,50]. The success in this case was dependent upon the acquisition of a large set of multiple reference FRF data. Finally, while not presented in this paper, extensive numerical examples, by one of the authors, have been run evaluating the effectiveness of this approach for various noise, modal density, and relative model order conditions [42].

7. Conclusions

The recognition of the equivalent importance of the numerator and denominator polynomials of a rational fraction polynomial has led to the development of a generalized residual model that has been shown to have broad application to frequency domain modal parameter estimation. Its inclusion in the UMPA formulation provides significant additional tools for identifying consistent modal parameters without the traditional additional work of eliminating computational poles. Additionally, when combined with a single reference rational fraction polynomial (RFP) algorithm, it allows the development of an efficient global pole and residue vector s.d.o.f. parameter estimation algorithm. Experience has shown that the generalized residuals, s.d.o.f. algorithm is superior to other s.d.o.f. algorithms, providing improved pole and vector estimates, and with appropriate programmatic implementation, requiring minimal additional computational time or resources.

Appendix A. Nomenclature

A^*	complex conjugate of A
A_r	residue of a single-input/single-output frequency response function of mode r
$[A_r]$	residue matrix of mode r
$[H(\omega)]$	frequency response function matrix
j	$\sqrt{-1}$
$\bar{m}$	maximum index of denominator polynomial, for all system modes
m	maximum index of denominator polynomial, for in-band modes
n_l	lower index limit of the residual polynomial
n_u	upper index limit of the residual polynomial
$\bar{N}$	total number of system modes
N	number of modes in the frequency range of interest
r	mode number (subscript)
R_k	kth order generalized residual polynomial coefficient

$[R_k]$ kth order generalized residual polynomial coefficient matrix
$[\hat{R}_k]$ kth order generalized residual polynomial coefficient matrix convolved with denominator polynomial
$[R_l(\omega)]$ lower residual function
$[R_u(\omega)]$ upper residual function
$[R_{l,k}]$ kth order lower residual polynomial coefficient matrix
$[R_{u,k}]$ kth order upper residual polynomial coefficient matrix
α_k kth order denominator polynomial coefficient
$[\alpha_k]$ kth order denominator polynomial coefficient matrix
β_k kth order numerator polynomial coefficient
$[\beta_k]$ kth order numerator polynomial coefficient matrix
$[\hat{\beta}_k]$ kth order numerator polynomial coefficient matrix combined with generalized residual polynomial
λ_r complex pole of mode r; $\lambda_r = \sigma_r + j\omega_r$
σ_r damping of mode r
ω variable of frequency (rad/s)
ω_r damped natural frequency of mode r

References

[1] R.J. Allemang, D.L. Brown, A unified matrix polynomial approach to modal identification, Journal of Sound and Vibration 211 (3) (1998) 301–322.
[2] M.H. Richardson, D.L. Formenti, Parameter estimation from frequency response measurements using rational fraction polynomials, Proceedings of the First International Modal Analysis Conference, Society of Experimental Mechanics, Bethel, CT, 1982, pp. 167–181.
[3] J.M. Leuridan, J.A. Kundrat, Advanced matrix methods for experimental modal analysis: a multi-matrix method for direct parameter estimation, Proceedings of the First International Modal Analysis Conference, Society of Experimental Mechanics, Bethel, CT, 1982, pp. 192–200.
[4] J.G. Gimenez, L.I. Carrascosa, Global fitting: an efficient method of experimental modal analysis of mechanical systems, Proceedings of the First International Modal Analysis Conference, Society of Experimental Mechanics, Bethel, CT, 1982, pp. 528–533.
[5] L. Petrick, Obtaining global frequency and damping estimates using single degree-of-freedom real mode methods, Proceedings of the Second International Modal Analysis Conference, Society of Experimental Mechanics, Bethel, CT, 1984, pp. 425–431.
[6] M.H. Richardson, D.L. Formenti, Global curve fitting of frequency response measurements using the rational fraction polynomial method, Proceedings of the Third International Modal Analysis Conference, Society of Experimental Mechanics, Bethel, CT, 1985, pp. 390–397.
[7] M.H. Richardson, Global frequency & damping estimates from frequency response measurements, Proceedings of the Fourth International Modal Analysis Conference, Society of Experimental Mechanics, Bethel, CT, 1986, pp. 465–470.
[8] H. Van der Auweraer, J. Leuridan, Multiple input orthogonal polynomial parameter estimation, Proceedings of the Fifth International Modal Analysis Conference, Society of Experimental Mechanics, Bethel, CT, 1987, pp. 986–994.
[9] D.K. Gustaveson, Direct parameter identification from frequency response measurements, Proceedings of the Fifth International Modal Analysis Conference, Society of Experimental Mechanics, Bethel, CT, 1987, pp. 1352–1356.
[10] K. Shye, C. Van Karsen, M. Richardson, Modal testing using multiple references, Proceedings of the Fifth International Modal Analysis Conference, Society of Experimental Mechanics, Bethel, CT, 1987, pp. 1407–1416.
[11] P. Ebersbach, H. Irretier, On the application of modal parameter estimation using frequency domain algorithms, The International Journal of Analytical and Experimental Modal Analysis 4 (4) (1989) 109–116.

[12] C.Y. Shih, Y.G. Tsuei, R.J. Allemang, D.L. Brown, A frequency domain global parameter estimation method for multiple reference frequency response measurements, Proceedings of the Sixth International Modal Analysis Conference, Society of Experimental Mechanics, Bethel, CT, 1988, pp. 389–396.
[13] Y.S. Wei, R.G. Smiley, R.C. Sohaney, A global frequency domain rational fraction orthogonal polynomial curve fit, Proceedings of the Sixth International Modal Analysis Conference, Society of Experimental Mechanics, Bethel, CT, 1988, pp. 1648–1654.
[14] F. Lembregts, J. Leuridan, Frequency domain direct parameter identification for modal analysis: state space formulation, Proceedings of the Seventh International Modal Analysis Conference, Society of Experimental Mechanics, Bethel, CT, 1989, pp. 1271–1277.
[15] W.B. Jeong, A. Nagamatsu, A new method for poly-reference identification of modal parameters in modal testing, Proceedings of the 10th International Modal Analysis Conference, Society of Experimental Mechanics, Bethel, CT, 1992, pp. 153–158.
[16] K. Kochersberger, L.D. Mitchell, A method for determining modal parameters using FRF curve-fitting and off-resonance sine dwell, Proceedings of the 10th International Modal Analysis Conference, Society of Experimental Mechanics, Bethel, CT, 1992, pp. 757–763.
[17] X. Keqin, Using the imaginary-part of FRF for modal identification and IRF estimation, Proceedings of the 10th International Modal Analysis Conference, Society of Experimental Mechanics, Bethel, CT, 1992, pp. 1431–1437.
[18] E. Chatelet, J. Piranda, Modal identification by squared amplitude fitting methods, Proceedings of the 13th International Modal Analysis Conference, Society of Experimental Mechanics, Bethel, CT, 1995, pp. 40–46.
[19] E. Balmes, Frequency domain identification of structural dynamics using the pole/residue parametrization, Proceedings of the 14th International Modal Analysis Conference, Society of Experimental Mechanics, Bethel, CT, 1996, pp. 540–546.
[20] T.M. Dahling, R.J. Allemang, A.W. Phillips, Application of differencing to frequency domain parameter estimation algorithms, Proceedings of the 17th International Modal Analysis Conference, Society of Experimental Mechanics, Bethel, CT, 1999, pp. 833–839.
[21] S. Braun, Y. Ram, Time and frequency identification methods in overdetermined systems, Mechanical Systems and Signal Processing 1 (3) (1987) 245–257.
[22] H. Van der Auweraer, J. Leuridan, Multiple input orthogonal polynomial parameter estimation, Mechanical Systems and Signal Processing 1 (3) (1987) 259–272.
[23] C.Y. Shih, Y.G. Tsuei, R.J. Allemang, D.L. Brown, A frequency domain global parameter estimation method for multiple reference frequency response measurements, Mechanical Systems and Signal Processing 2 (4) (1988) 349–366.
[24] D.L. Brown, R.J. Allemang, R.J. Zimmerman, M. Mergeay, Parameter estimation techniques for modal analysis, SAE Paper Number 790221, SAE Transactions, 88 (1979) 828–846.
[25] F. Deblauwe, C.Y. Shih, R.W. Rost, D.L. Brown, Survey of modal parameter estimation algorithms applicable to spatial domain sine testing, Proceedings of the 12th International Seminar on Modal Analysis, Katholieke Universiteit Leuven, Leuven, Belgium, 1987.
[26] H. Van der Auweraer, R. Snoeys, J.M. Leuridan, A global frequency domain parameter estimation technique for mini-computers, Proceedings of the 10th International Seminar on Modal Analysis, Society of Experimental Mechanics, Bethel, CT, 1985.
[27] S.M. Crowley, D.L. Brown, R.J. Allemang, The extraction of valid residue terms using the polyreference technique, Proceedings of the Third International Modal Analysis Conference, Society of Experimental Mechanics, Bethel, CT, 1985, pp. 80–87.
[28] J. Leuridan, J. Lipkens, H. Van der Auweraer, F. Lembgrets, Global modal parameter estimation methods: an assessment of time versus frequency domain implementation, Proceedings of the Fourth International Modal Analysis Conference, Society of Experimental Mechanics, Bethel, CT, 1986, pp. 1586–1595.
[29] R.L. Mayes, A multi-degree-of-freedom mode shape estimation algorithm using quadrature response, Proceedings of the 11th International Modal Analysis Conference, Society of Experimental Mechanics, Bethel, CT, 1993, pp. 1026–1034.
[30] K. Kochersberger, L.D. Mithcell, The use of an improved residual model and sine excitation to iteratively determine mode vectors, Proceedings of the 12th International Modal Analysis Conference, Society of Experimental Mechanics, Bethel, CT, 1994, pp. 356–262.

[31] M.A. Lamontia, On the determination and use of residual flexibilities, inertia restraints and rigid body modes, Proceedings of the First International Modal Analysis Conference, Society of Experimental Mechanics, Bethel, CT, 1982, pp, 152–159.
[32] B.A. Brinkman, Generating modal parameters that compensate for residual energy, Proceedings of the Fourth International Modal Analysis Conference, Society of Experimental Mechanics, Bethel, CT, 1986, pp. 119–122.
[33] B.A. Brinkman, A quantitative study using residual modes to improve dynamic models, Proceedings of the Fifth International Modal Analysis Conference, Society of Experimental Mechanics, Bethel, CT, 1987, pp. 671–678.
[34] M.L.M. Duarte, D.J. Ewins, High-frequency pseudo-mode approximation for high frequency residual terms, Proceedings of the 14th International Modal Analysis Conference, Society of Experimental Mechanics, Bethel, CT, 1996, pp. 261–266.
[35] M.L.M. Duarte, D.J. Ewins, Mass-residual approach for the compensation of high-frequency residual terms, Proceedings of the 15th International Modal Analysis Conference, Society of Experimental Mechanics, Bethel, CT, 1997, pp. 2038–2043.
[36] N. Okubo, T. Matsuzaki, The effect of inertia restraint and residual flexibility on the accuracy of structural modification, Proceedings of the 13th International Seminar on Modal Analysis, Society of Experimental Mechanics, Bethel, CT, 1988.
[37] M.L.M. Duarte, D.J. Ewins, Experimental estimation of high-frequency residual term based on two extra parameters, Proceedings of the 21st International Seminar on Modal Analysis, Society of Experimental Mechanics, Bethel, CT, 1996, pp. 1277–1286.
[38] I. Ahmed, G.R. Tomlinson, Reducing the effects of residual modes in measured frequency–response data, The International Journal of Analytical and Experimental Modal Analysis 2 (3) (1987) 113–120.
[39] A. Klosterman, On the Experimental Determination and Use of Modal Representations of Dynamic Characteristics, Doctoral Dissertation, University of Cincinnati, 1971, 184pp.
[40] P. Van Loon, Modal Parameters of Mechanical Structures, Doctoral Dissertation, Katholieke Universiteit of Leuven, Leuven, Belgium, 1974.
[41] R.J. Allemang, Vibrations: analytical and experimental moda1 analysis, Chapter 6—Modal parameter estimation, UC-SDRL-CN-20-263-662, University of Cincinnati, February 1998, 96pp.
[42] W.A. Fladung, A Generalized Residuals Model for the Unified Matrix Polynomial Approach to Frequency Domain Modal Parameter Estimation, Doctoral Dissertation, University of Cincinnati, 2001, 146pp.
[43] R.J. Allemang, D.L. Brown, A review of modal parameter estimation concepts, Proceedings of the 11th International Seminar on Modal Analysis, Katholieke Universiteit Leuven, Leuven, Belgium, 1986.
[44] A.W. Phillips, R.J. Allemang, W.A. Fladung, The complex mode indicator function (CMIF) as a parameter estimation algorithm, Proceedings of the 16th International Modal Analysis Conference, Society of Experimental Mechanics, Bethel, CT, 1998.
[45] C.Y. Shih, Y.G. Tsuei, R.J. Allemang, D.L. Brown, Complex mode indication function and its applications to spatial domain parameter estimation, Mechanical Systems and Signal Processing 2 (4) (1988) 367–377.
[46] W.A. Fladung, The Development and Implementation of Multiple Reference Impact Testing, Masters Thesis, University of Cincinnati, 1994, 191pp.
[47] R.J. Allemang, The modal assurance criterion (MAC): twenty years of use and abuse, Proceedings of the 20th International Modal Analysis Conference, Society of Experimental Mechanics, Bethel, CT, 2002, pp. 397–405.
[48] A.W. Phillips, R.J. Allemang, The enhanced frequency response function (eFRF): scaling and other issues, Proceedings of the 23rd International Seminar on Modal Analysis, Katholieke Universiteit Leuven, Leuven, Belgium, 1998, pp. 385–392.
[49] W.A. Fladung, A.W. Phillips, D.L. Brown, Specialized parameter estimation algorithms for multiple reference impact testing, Proceedings of the 15th International Modal Analysis Conference, Society of Experimental Mechanics, Bethel, CT, 1997.
[50] F.N. Catbas, M. Lenett, D.L. Brown, S.W. Doebling, C.R. Farrar, A. Turer, Modal analysis of multi-reference impact test data of steel stringer bridges, Proceedings of the 15th International Modal Analysis Conference, Society of Experimental Mechanics, Bethel, CT, 1997.